Nonlinear Dynamics (2005) 42: 347–369 

# An Internal Damping Model for the Absolute Nodal Coordinate Formulation

D. GARCÍA-VALLEJO*, J. VALVERDE, and J. DOMÍNGUEZ
*Department of Mechanical and Materials Engineering, University of Seville, Camino de los descubrimientos s/n, 41092 Seville, Spain; *Author for correspondence (e-mail: dgvallejo@us.es; fax: +34-954-48 7295)*

(Received: 8 February 2005; accepted: 20 April 2005)

**Abstract.** Introducing internal damping in multibody system simulations is important as real-life systems usually exhibit this type of energy dissipation mechanism. When using an inertial coordinate method such as the absolute nodal coordinate formulation, damping forces must be carefully formulated in order not to damp rigid body motion, as both this and deformation are described by the same set of absolute nodal coordinates. This paper presents an internal damping model based on linear viscoelasticity for the absolute nodal coordinate formulation. A practical procedure for estimating the parameters that govern the dissipation of energy is proposed. The absence of energy dissipation under rigid body motion is demonstrated both analytically and numerically. Geometric nonlinearity is accounted for as deformations and deformation rates are evaluated by using the Green–Lagrange strain–displacement relationship. In addition, the resulting damping forces are functions of some constant matrices that can be calculated in advance, thereby avoiding the integration over the element volume each time the damping force vector is evaluated.

**Key words:** absolute nodal coordinates, flexible multibody dynamics, internal damping

## 1. Introduction

The importance of damping in mechanical engineering is well known. Almost every mechanical system experiences some damping arising from various sources. For instance, mechanism and machine joints develop friction and damping to an extent dependent on the way connections are designed. Bearing supports in rotordynamics introduce so-called "external damping" in the system. Proper operation of the rotor occasionally depends strongly on the way such damping has been modelled at the machine design stage. There is also "internal damping", which results from the hysteresis loops some materials undergo when subjected to alternative stresses. In the past, machines and mechanisms were designed on the assumption that the different parts of the system would all be rigid. Therefore, no internal damping had to be modelled. In recent years, the complexity of machine solicitation (high-speed machines, very flexible and light components, etc.), requires that some parts or even the whole machine be assumed flexible in order to obtain realistic simulated results. In order to ensure adequate accuracy, the flexibility of the system and the way the different parts of the machine dissipate energy through hysteresis loops should therefore be properly modelled.

Because the hysteretic damping effect is generally small relative to all other damping effects arising in a machine, it should be considered when one or more of the following conditions occur:

- The mechanism operates in vacuum, so no damping due to aerodynamic drag is to be expected.
- Hysteretic damping is significant (e.g. in plasticized materials) as compared to all other damping forms in the machine (damping in the joints, etc.).
- Hysteretic damping governs the dynamics of the system.

As stated above, internal damping controls the dynamic behavior of the system in some cases. Such is the case with the Short Electrodynamic Tether (SET) problem studied by Valverde et al. [1]. In this system, a long rod with a tiny cross-section is rotated about its longitudinal axis in outer space (vacuum). The motion is transferred by torsion to the whole system. This problem is similar to that of an unbalanced rotor except that large deformations are expected. In such a case, in the absence of other damping sources, aerodynamic drag and joints generating damping, hysteretic damping can be substantial. If the system is modelled without consideration of hysteretic damping, this configuration is stable at any angular velocity applied to the system. On the other hand, because the rod may suffer alternative stresses, the model should incorporate internal damping. In such a case, the system seems to be unstable above an angular velocity called the "critical velocity", which is approximately equal to the first bending natural frequency of the system. Modelling internal damping is therefore essential to accurately reproduce the behavior of the system. It has been proven in [1] also, the dynamics of the system above the critical velocity is governed by geometric nonlinearity in the thin rod. It is therefore essential to construct a geometrically nonlinear internal damping force model.

Hysteretic damping can also be important in checking a dynamic flexible model against experimental data when hysteretic damping is substantial. Under these considerations, the results can be rather disparate unless an appropriate internal damping force model is introduced in the simulation procedure as it is almost impossible to eliminate dissipation from the prototype in the laboratory.

A number of formulations have been developed over the past 30 years to account for flexible parts in mechanisms. One of the most frequently used is called the Floating Reference Frame approach [2, 3], which considers small deformations measured from a floating frame that describes rigid body motions and is connected to the body via a set of reference conditions. When large deformations occur in the flexible parts of the mechanism, the previous formulations are no longer appropriate. In such a case, geometric nonlinearity must be taken into account in order to properly manage such deformations. Several formulations have recently been developed in order to improve the simulation stage of these problems. One is the Large Rotation Vector approach, proposed by Simo and Vu-Quoc [4], this is a finite element-like approach used in some finite element commercial packages. It uses global positions of the finite element nodes and an incremental procedure to update nodal rotations. One other approach frequently used to analyze large deformations is the Absolute Nodal Coordinate formulation (ANCF) [2, 5], which uses global displacements and slopes of the finite element nodes, so no rotation or incremental procedure is needed. This formulation produces a constant mass matrix, so no Coriolis or centrifugal forces are involved. However, it generates a highly nonlinear coordinate-dependent elastic force vector. This formulation is quite recent, so it has generated little literature on damping. Takahashi et al. [6] introduced a Rayleigh proportional damping matrix on the assumption that deformations within each finite element are small. Also, the nodal coordinates are split into two groups that are used to characterize rigid body motions and small deformations, respectively. The latter can be expressed as the product of a constant stiffness matrix and a small deformation set of coordinates when computing bending forces. Axial forces cannot be simplified in this way owing to the structure of the elastic forces involved [6]. At this point, the constant mass matrix and the constant bending stiffness matrix are used to evaluate the proportional damping matrix. With this procedure, no large deformations within an individual element can be considered; otherwise, the damping forces are inaccurately evaluated (their calculation is based on the assumption that deformations within each finite element are small) and, more importantly, rigid body motions in the element are also damped. The simplified elastic force vector used elsewhere [6] resolves axial and bending deformations, which is unfeasible with large deformations. Therefore, computing large deformations in the previous formulation entails using a vast number of finite elements. Yoo et al. [7] used a proportional damping approach to model external damping and checked their results

against experimental data. They found a good consistency even with large oscillations in a cantilever beam. The number of elements for small oscillations was fairly small but that for large oscillations was considerably increased. In addition, large oscillations do not necessarily imply large deformations [8], so, strictly speaking, this method has not been experimentally checked with large deformations, but only with large displacements and rotations in different sections of the beam.

Shabana and co-workers [9, 10] developed a continuum mechanics approach to compute the elastic forces in a straightforward, unique manner for any finite element in the ANCF (2D/3D beams and plates). The model allows large deformations to be considered within every finite element, so simulating large deformation does not require the use of a vast number of finite elements. An internal damping force model based on the continuum mechanics approach would be more useful, straightforward and accurate than the previous methods [6, 7] with a view to modelling internal damping. For this purpose, the hysteretic material must be assimilated to an equivalent viscoelastic material (Kelvin-Voigt law [11]). This approximation is widely used in the field of mechanical vibrations.

In this work, we developed one such internal damping model for generic finite element systems (viz. 3D beams and plates). In order to efficiently evaluate the damping forces involved, an invariant-based algorithm similar to a previous one presented in [12] for elastic forces was developed. As shown elsewhere [12], the computational cost of the simulations can be considerably decreased.

This paper is structured as follows: Section 2 provides a background on the absolute nodal coordinate formulation in relation to the continuum mechanics approach. Section 3 explains the formulation of the continuum mechanics-based internal damping forces. Section 4 demonstrates a salient feature of this formulation: rigid body motions induce no dissipation. Section 5, discusses several examples of problems that are tested analytically and by comparison with other, well-established methods. Finally, some interesting conclusions are drawn and future projects are outlined.

## 2. Background on Absolute Nodal Coordinate Formulation

The absolute nodal coordinate formulation is a non-incremental nonlinear finite element procedure for studying flexible bodies that experience large rotations and large deformations [5]. All nodal coordinates, which include the global positions of nodes and global slopes, are referred to an inertial frame. Hence, the nodal variables contain the information of rigid body motions and deformations. In this formulation, the global position of an arbitrary point in element $j$ of body $i$ is interpolated as follows:

$$\mathbf{r}^{ij} = \mathbf{S}^{ij}\mathbf{e}^{ij}, \tag{1}$$

where $\mathbf{S}^{ij}$ is the shape function for element $ij$ and $\mathbf{e}^{ij}$ the element coordinate vector. Each element coordinate vector contains a set of nodal coordinate vectors. For instance, beam elements formulated with two nodes contain two nodal coordinate vectors [9, 10], that is, there is a coordinate vector associated to each element node. Thus, node $k$ of element $j$ in body $i$ (Figure 1) is defined by the following vector

$$\mathbf{e}^{ijk} = \left[\mathbf{r}^{ijk\mathrm{T}} \quad \frac{\partial \mathbf{r}}{\partial x}^{ijk\mathrm{T}} \quad \frac{\partial \mathbf{r}}{\partial y}^{ijk\mathrm{T}} \quad \frac{\partial \mathbf{r}}{\partial z}^{ijk\mathrm{T}}\right]^{\mathrm{T}}, \tag{2}$$

where $\mathbf{r}^{ijk\mathrm{T}}$ is the global position vector of node $ijk$, and $x$, $y$ and $z$ are the element parameters in the undeformed configuration. For a quadrilateral plate/shell element [13], the element coordinate vector contains four nodal coordinate vectors. If the nodes are designated $k$, $l$, $m$ and $n$, then the element

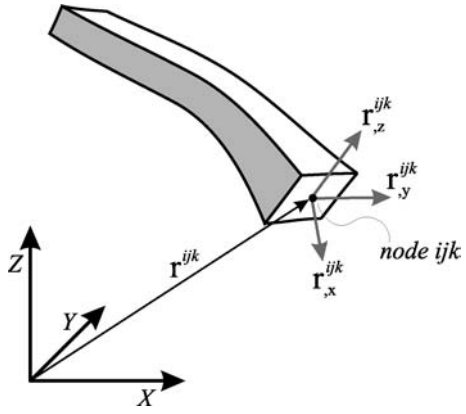


*Figure 1.* Nodal coordinates in a deformed beam element.

coordinate vectors can be expressed as

$$\mathbf{e}^{ij} = \left[\mathbf{e}^{ijk\mathrm{T}} \quad \mathbf{e}^{ijl\mathrm{T}} \quad \mathbf{e}^{ijm\mathrm{T}} \quad \mathbf{e}^{ijn\mathrm{T}}\right]^{\mathrm{T}}. \tag{3}$$

Equations of motion for the element are typically obtained by using analytical mechanics methods such as those based on Lagrange equations. The kinetic energy can be calculated in a very straightforward manner that produces a constant mass matrix thanks to use of inertial coordinates [2]. By using the isoparametric property of the element, the kinetic energy can be integrated in a regular domain as follows

$$T = \frac{1}{2}\int_{V_\mathrm{e}} \rho\, \dot{\mathbf{r}}^{\mathrm{T}}\dot{\mathbf{r}}\, dV_\mathrm{e} = \frac{1}{2}\int_{V} \rho\, \dot{\mathbf{r}}^{\mathrm{T}}\dot{\mathbf{r}}\, |\mathbf{J}|\, dV, \tag{4}$$

where $\rho$ is the material density, $V_\mathrm{e}$ the volume of the element, $V$ that in an undeformed configuration and $|\mathbf{J}|$ the Jacobian of the mapping between the reference and a straight configuration. The use of the mapping allows one to perform the integration over a regular straight domain. The elastic energy can be evaluated via a continuum mechanics approach, using the nonlinear Green–Lagrange strain–displacement relationship to account for nonlinear effects. Thus, the elastic energy is integrated as follows:

$$U = \frac{1}{2}\int_{V_\mathrm{e}} \boldsymbol{\sigma} : \varepsilon\, dV_\mathrm{e} = \frac{1}{2}\int_{V} \boldsymbol{\sigma} : \varepsilon\, |\mathbf{J}|\, dV, \tag{5}$$

where $\boldsymbol{\sigma}$ is the second Piola–Kirchhoff stress tensor and $\varepsilon$ the Green–Lagrange strain tensor. The strain tensor can be expressed as

$$\varepsilon = \frac{1}{2}\left[\frac{\partial \mathbf{r}}{\partial \mathbf{r}_0}^{\mathrm{T}}\frac{\partial \mathbf{r}}{\partial \mathbf{r}_0} - \mathbf{I}\right], \tag{6}$$

where $\mathbf{r}_0$ is the location of an arbitrary material point (i.e. a point in the reference configuration). By using the chain rule and the mapping between the real configuration and the straight configuration, the strain tensor can be shown to only involve first-order derivatives with respect to coordinates in the undeformed configuration:

$$\frac{\partial \mathbf{r}}{\partial \mathbf{r}_0} = \frac{\partial \mathbf{r}}{\partial \mathbf{x}}\left[\frac{\partial \mathbf{r}_0}{\partial \mathbf{x}}\right]^{-1}, \tag{7}$$

where

$$\frac{\partial \mathbf{r}}{\partial \mathbf{x}} = \left[\mathbf{S}_{,x}\mathbf{e} \quad \mathbf{S}_{,y}\mathbf{e} \quad \mathbf{S}_{,z}\mathbf{e}\right], \tag{8}$$

and

$$\frac{\partial \mathbf{r}_0}{\partial \mathbf{x}} = \left[\mathbf{S}_{,x}\mathbf{e}_0 \quad \mathbf{S}_{,y}\mathbf{e}_0 \quad \mathbf{S}_{,z}\mathbf{e}_0\right]. \tag{9}$$

In Equations (8) and (9), $\mathbf{S}_{,\alpha} = \partial\mathbf{S}/\partial\alpha$ ($\alpha = x, y, z$) is used to denote the partial derivative of the shape function $\mathbf{S}$ with respect to parameter $\alpha$. The nodal coordinate vector, $\mathbf{e}_0$ describes the reference configuration. Note that all stresses in the reference configuration, which can be curved or straight, are zero. Elastic deformations can be expressed as follows [12]:

$$\begin{gathered}\varepsilon_{11} = \frac{1}{2}\left(\mathbf{e}^{\mathrm{T}}\mathbf{S}_{,1}{}^{\mathrm{T}}\mathbf{S}_{,1}\mathbf{e} - 1\right) \quad \varepsilon_{22} = \frac{1}{2}\left(\mathbf{e}^{\mathrm{T}}\mathbf{S}_{,2}{}^{\mathrm{T}}\mathbf{S}_{,2}\mathbf{e} - 1\right) \quad \varepsilon_{33} = \frac{1}{2}\left(\mathbf{e}^{\mathrm{T}}\mathbf{S}_{,3}{}^{\mathrm{T}}\mathbf{S}_{,3}\mathbf{e} - 1\right) \\ \varepsilon_{12} = \frac{1}{2}\mathbf{e}^{\mathrm{T}}\mathbf{S}_{,1}{}^{\mathrm{T}}\mathbf{S}_{,2}\mathbf{e} \qquad \varepsilon_{13} = \frac{1}{2}\mathbf{e}^{\mathrm{T}}\mathbf{S}_{,1}{}^{\mathrm{T}}\mathbf{S}_{,3}\mathbf{e} \qquad \varepsilon_{23} = \frac{1}{2}\mathbf{e}^{\mathrm{T}}\mathbf{S}_{,2}{}^{\mathrm{T}}\mathbf{S}_{,3}\mathbf{e}\end{gathered}, \tag{10}$$

where the subscript "$\alpha$" denotes partial derivative with respect to $\mathbf{r}_{0_\alpha}$ ($\alpha = 1, 2, 3$). As shown elsewhere [12], the elastic force vector can be evaluated as a function of a set of constant matrices that are integrated once in advance at the pre-processing stage.

## 3. Formulation of Damping Forces

Accounting for the damping effect is an important issue in multibody systems as every mechanism in real life exhibits some dissipation of energy from various sources. Some approaches [6, 7] have been successfully used to account for dissipation arising from an external source such as friction with a circumventing fluid. However, such approaches fail to reproduce internal damping as rigid body motions are also damped. Thus, an effective model for internal damping should dissipate energy only if the system experiences some deformation, i.e. damping forces should be zero for every undeformed configuration of the system. This issue is addressed later on.

Proportional damping makes sense when modal mass and stiffness matrices are available; however, this is not the case with many multibody system formulations, such as ANCF. Moreover, if one fails to provide a means for separating motion due to deformation from global motion, then the model will damp the rigid body motions of the system [6].

### 3.1. Obtaining Damping Forces from a Rayleigh Dissipation Function

One of the most widely used approaches for introducing damping into a system is the development of a Rayleigh dissipation function. Such a function allows systematic derivation of dissipative forces by partial differentiation with respect to the generalized velocities. The idea behind the dissipation function comes from the virtual work done by damping forces as shown in this section. If one assumes damping forces to be proportional to the velocity and to act in opposite direction as the velocity vector, then

$$\mathbf{F} = -c\dot{\mathbf{r}}, \tag{11}$$

where $\mathbf{F}$ is the damping force vector and $c$ can be a function of $\mathbf{r}$ in general. The virtual work done by these forces can be calculated by integrating over the solid volume:

$$\delta W = \int_{V_e} \mathbf{F}\delta\mathbf{r}\, dV_e = \int_{V_e} \mathbf{F} \sum_{i=1}^{n} \frac{\partial \mathbf{r}}{\partial q_i}\delta q_i\, dV_e = \sum_{i=1}^{n} Q_i \delta q_i, \tag{12}$$

where $q_i$ $(i = 1, 2, \ldots, n)$ are the generalized coordinates of the system. Equation (11) can be used together with the following relation

$$\frac{\partial \mathbf{r}}{\partial q_i} = \frac{\partial \dot{\mathbf{r}}}{\partial \dot{q}_i}, \tag{13}$$

in order to obtain a closed expression for the Rayleigh function [14]. Thus, one can define the generalized damping forces of Equation (12) as follows:

$$Q_i = -\frac{\partial F_d}{\partial \dot{q}_i}, \tag{14}$$

where $F_d$ is the Rayleigh dissipation function, which has units of power, and can be written as

$$F_d = \frac{1}{2}\int_{V_e} c\dot{\mathbf{r}}^2\, dV_e. \tag{15}$$

The Rayleigh function is a quadratic function of the velocities and, in general, can be dependent on the position as $c$ can vary from point to point within the solid. Equation (15) assumes that the motion of one point does not lead to a dissipative force on another point. There is no need to impose this restriction, so more general Rayleigh functions can be defined. In this work, we used this approach to develop an appropriate Rayleigh function for obtaining consistent damping forces.

### 3.2. Damping Forces in the Absolute Nodal Coordinate Formulation

Internal damping models for beams or plates in the field of vibrations, are usually based on viscoelasticity concepts [15]. Such models are designed for simple stress states such as bending or torsion by including a dissipation factor. However, damping models based on linear viscoelastic relations can be generalized to multiaxial stress states. One should bear in mind that the response of materials to deviatoric and dilatational excitations are different and so should be the dissipation factors relating tensions and time derivatives of strains as a result [16]. For this reason, we used the following relation in the model:

$$\begin{aligned} s_{ij} &= 2Gd_{ij} + 2G\gamma_d \dot{d}_{ij} \\ \sigma_{ii} &= 3K\varepsilon_{ii} + 3K\gamma_s \dot{\varepsilon}_{ii} \end{aligned}, \tag{16}$$

where $s_{ij}$ and $d_{ij}$ are the deviatoric stress and strain tensors, $G$ the shear modulus of the material, $\sigma_{ii}$ and $\varepsilon_{ii}$ are the dilatational stress and strain, respectively, $K$ the bulk modulus of the material, and the over-dot denotes time derivative. $\gamma_s$ and $\gamma_d$ in Equation (16) are the dissipation factors associated to dilatational and deviatoric stresses, respectively.

The deviatoric stress tensor can be obtained by differentiating the volume-preserving part of the strain energy with respect to Cauchy–Green strain tensor as explained in [17]. When a material description is used, as it is the case of the internal force model used in this paper, the expression of the deviatoric and volumetric tensors are rather involved. However, large strains do not often appear in most of multibody

system dynamics applications. It is reasonable, in such a case, to assume a simpler description of the deviatoric part of the stress and strain tensors as follows:

$$\begin{aligned}\sigma_{ij} &= \frac{1}{3}\,\sigma_{ii}\delta_{ij} + s_{ij},\\ \varepsilon_{ij} &= \frac{1}{3}\,\varepsilon_{ii}\delta_{ij} + d_{ij}.\end{aligned} \tag{17}$$

The use of Equation (17) confines the model to the case of large rotations and large deformations but small strains, which in fact is very common in multibody applications. If large strains are expected, exact expressions for the deviatoric and the volumetric components are required [17, 18]. According to Equation (17), the constitutive equations can be written as follows:

$$\sigma_{ij} = \underbrace{2G\varepsilon_{ij} + \left(K - \frac{2G}{3}\right)\varepsilon_{ii}\delta_{ij}}_{\text{elastic}} + \underbrace{2G\gamma_{\mathrm{d}}\dot{\varepsilon}_{ij} + \left(K\gamma_{\mathrm{s}} - \frac{2G\gamma_{\mathrm{d}}}{3}\right)\dot{\varepsilon}_{ii}\delta_{ij}}_{\text{viscous}}, \tag{18}$$

where $\delta_{ij}$ is the Kronecker delta function. The dissipated power, $P_{\mathrm{d}}$, can be calculated in the same manner as the strain energy. Thus, the part of the stress tensor corresponding to damping is multiplied by the time derivative of the strain tensor to obtain the power dissipated per unit volume:

$$P_{\mathrm{d}} = \frac{1}{2}\int_{V_{\mathrm{e}}} \boldsymbol{\sigma}_{\text{viscous}} : \dot{\boldsymbol{\varepsilon}}\, dV_{\mathrm{e}} = \frac{1}{2}\int_{V} \boldsymbol{\sigma}_{\text{viscous}} : \dot{\boldsymbol{\varepsilon}}\, |\mathbf{J}|\; dV. \tag{19}$$

Recalling Equations (10), it is easy to see that the time-derivative of the strains can be written as follows:

$$\dot{\varepsilon}_{ij} = \frac{1}{2}\dot{\mathbf{e}}^{\mathrm{T}}\left(\mathbf{S}_{,i}^{\mathrm{T}}\mathbf{S}_{,j} + \mathbf{S}_{,j}^{\mathrm{T}}\mathbf{S}_{,i}\right)\mathbf{e} \quad (i, j = 1, 2, 3). \tag{20}$$

Substituting Equation (20) into Equation (19) reveals that the dissipated power is a quadratic form of the generalized velocity vector. In the following expression, the dissipated power in Equation (19) has been assumed to be a Rayleigh function and damping forces obtained by partial differentiation with respect to $\dot{\mathbf{e}}$:

$$\mathbf{Q}_{\mathrm{d}} = -\left(\frac{\partial P_{\mathrm{d}}}{\partial \dot{\mathbf{e}}}\right)^{\mathrm{T}}. \tag{21}$$

The corresponding expression for an arbitrary flexible element is

$$\begin{aligned}\mathbf{Q}_{\mathrm{d}} = -\frac{1}{2}\int_{V_{\mathrm{e}}} \Bigg[ &\left(K\gamma_{\mathrm{s}} + \frac{4G\gamma_{\mathrm{d}}}{3}\right)\left(2\dot{\varepsilon}_{11}\frac{\partial \dot{\varepsilon}_{11}}{\partial \dot{\mathbf{e}}}^{\mathrm{T}} + 2\dot{\varepsilon}_{22}\frac{\partial \dot{\varepsilon}_{22}}{\partial \dot{\mathbf{e}}}^{\mathrm{T}} + 2\dot{\varepsilon}_{33}\frac{\partial \dot{\varepsilon}_{33}}{\partial \dot{\mathbf{e}}}^{\mathrm{T}}\right)\\ &+ 4G\gamma_{\mathrm{d}}\left(2\dot{\varepsilon}_{12}\frac{\partial \dot{\varepsilon}_{12}}{\partial \dot{\mathbf{e}}}^{\mathrm{T}} + 2\dot{\varepsilon}_{13}\frac{\partial \dot{\varepsilon}_{13}}{\partial \dot{\mathbf{e}}}^{\mathrm{T}} + 2\dot{\varepsilon}_{23}\frac{\partial \dot{\varepsilon}_{23}}{\partial \dot{\mathbf{e}}}^{\mathrm{T}}\right) + \left(2K\gamma_{\mathrm{s}} - \frac{4G\gamma_{\mathrm{d}}}{3}\right)\left(\dot{\varepsilon}_{11}\frac{\partial \dot{\varepsilon}_{22}}{\partial \dot{\mathbf{e}}}^{\mathrm{T}}\right.\\ &\left.+ \dot{\varepsilon}_{22}\frac{\partial \dot{\varepsilon}_{11}}{\partial \dot{\mathbf{e}}}^{\mathrm{T}} + \dot{\varepsilon}_{11}\frac{\partial \dot{\varepsilon}_{33}}{\partial \dot{\mathbf{e}}}^{\mathrm{T}} + \dot{\varepsilon}_{33}\frac{\partial \dot{\varepsilon}_{11}}{\partial \dot{\mathbf{e}}}^{\mathrm{T}} + \dot{\varepsilon}_{22}\frac{\partial \dot{\varepsilon}_{33}}{\partial \dot{\mathbf{e}}}^{\mathrm{T}} + \dot{\varepsilon}_{33}\frac{\partial \dot{\varepsilon}_{22}}{\partial \dot{\mathbf{e}}}^{\mathrm{T}}\right)\Bigg] dV_{\mathrm{e}} = -\mathbf{C}(\mathbf{e})\dot{\mathbf{e}},\end{aligned} \tag{22}$$

where $\mathbf{C}(\mathbf{e})$ is a coordinate-dependent matrix. At this point, there are two parameters, the dissipation factors, $\gamma_{\mathrm{s}}$ and $\gamma_{\mathrm{d}}$, that are left to be assigned a value. This issue is addressed in a subsequent section.

After simple algebraic manipulations, the damping matrix has the following expression

$$\mathbf{C}(\mathbf{e}) = \frac{1}{2}\int_{V_e}\left[\left(2K\gamma_s + \frac{8G\gamma_d}{3}\right)\left(\sum_{\alpha=1}^{3}\mathbf{S}_{,\alpha}^{T}\mathbf{S}_{,\alpha}\mathbf{e}\mathbf{e}^{T}\mathbf{S}_{,\alpha}^{T}\mathbf{S}_{,\alpha}\right)\right.$$
$$+2G\gamma_d\left(\sum_{\alpha=1}^{3}\sum_{\substack{\beta=1\\\beta\neq\alpha}}^{3}\mathbf{S}_{,\alpha}^{T}\mathbf{S}_{,\beta}\mathbf{e}\mathbf{e}^{T}\mathbf{S}_{,\alpha}^{T}\mathbf{S}_{,\beta}+\mathbf{S}_{,\alpha}^{T}\mathbf{S}_{,\beta}\mathbf{e}\mathbf{e}^{T}\mathbf{S}_{,\beta}^{T}\mathbf{S}_{,\alpha}\right)$$
$$\left.+\left(2K\gamma_s - \frac{4G\gamma_d}{3}\right)\left(\sum_{\alpha=1}^{3}\sum_{\substack{\beta=1\\\beta\neq\alpha}}^{3}\mathbf{S}_{,\alpha}^{T}\mathbf{S}_{,\alpha}\mathbf{e}\mathbf{e}^{T}\mathbf{S}_{,\beta}^{T}\mathbf{S}_{,\beta}\right)\right]dV_e. \tag{23}$$

The damping matrix results in a nonlinear function of the nodal coordinate vector. However, the large expression in Equation (23) does not require the integration over the volume of the element for each evaluation of the damping forces as the nodal coordinates can be factored out of the integrals. In fact, the ensuing expressions for the components of the damping matrix are polynomial functions of the nodal coordinates and their coefficients can be integrated in advance. Once done, the integral over the volume of the element will no longer be required. This way, evaluating the damping force requires only a few arithmetic operations.

3.2.1. *Evaluation of Damping Forces*

Damping forces should be evaluated in a systematic manner. Based on the form of the damping matrix in Equation (23) each of its components can be evaluated as a quadratic form of the nodal coordinate vector. To this end, component $ij$ in the product $\mathbf{A}\mathbf{e}\mathbf{e}^{T}\mathbf{B}$, where $\mathbf{A}$ and $\mathbf{B}$ are two arbitrary matrices, is developed as follows:

$$(\mathbf{A}\mathbf{e}\mathbf{e}^{T}\mathbf{B})_{ij} = \sum_{k}\sum_{l}A_{ik}e_k e_l B_{lj} = \mathbf{e}^{T}\mathbf{D}^{ij}\mathbf{e}, \tag{24}$$

where $\mathbf{D}^{ij}$ is a matrix built as the product of the transpose of row $i$ in matrix $\mathbf{A}$ and row $j$ in the transpose of matrix $\mathbf{B}$, i.e.

$$\mathbf{D}^{ij} = (\mathbf{A}_i)^{T}(\mathbf{B}^{T})_j, \tag{25}$$

$\mathbf{A}_i$ being row $i$ in matrix $\mathbf{A}$. By using Equations (24) and (25), the matrix $\mathbf{D}^{ij}$ corresponding to each term in the summation of Equation (23) can be added to obtain matrix $\mathbf{C}^{ij}$ as follows:

$$\mathbf{C}^{ij} = \frac{1}{2}\int_{V_e}\left[\left(2K\gamma_s + \frac{8G\gamma_d}{3}\right)\left(\sum_{\alpha=1}^{3}\left(\mathbf{S}_{,\alpha}^{T}\mathbf{S}_{,\alpha}\right)_i^{T}\left(\mathbf{S}_{,\alpha}^{T}\mathbf{S}_{,\alpha}\right)_j\right)\right.$$
$$+2G\gamma_d\left(\sum_{\alpha=1}^{3}\sum_{\substack{\beta=1\\\beta\neq\alpha}}^{3}\left(\mathbf{S}_{,\alpha}^{T}\mathbf{S}_{,\beta}\right)_i^{T}\left(\mathbf{S}_{,\beta}^{T}\mathbf{S}_{,\alpha}\right)_j+\left(\mathbf{S}_{,\alpha}^{T}\mathbf{S}_{,\beta}\right)_i^{T}\left(\mathbf{S}_{,\alpha}^{T}\mathbf{S}_{,\beta}\right)_j\right)$$
$$\left.+\left(2K\gamma_s - \frac{4G\gamma_d}{3}\right)\left(\sum_{\alpha=1}^{3}\sum_{\substack{\beta=1\\\beta\neq\alpha}}^{3}\left(\mathbf{S}_{,\alpha}^{T}\mathbf{S}_{,\alpha}\right)_i^{T}\left(\mathbf{S}_{,\beta}^{T}\mathbf{S}_{,\beta}\right)_j\right)\right]dV_e. \tag{26}$$

Matrix $\mathbf{C}^{ij}$ allows the coefficients of the damping matrix to be calculated as follows:

$$(\mathbf{C}(\mathbf{e}))_{ij} = \mathbf{e}^{\mathrm{T}}\mathbf{C}^{ij}\mathbf{e} \tag{27}$$

As stated above, these matrices are obtained by integrating over the volume of the element at the pre-processing stage and stored in order to evaluate the damping forces during the simulation stage. For this reason, matrices $\mathbf{C}^{ij}$ have been called invariant damping matrices. The matrix structure of the invariant allows the information required to evaluate the damping forces to be stored in a systematic manner. From Equation (23) it can be easily shown that the damping matrix is symmetric, so only invariant matrices corresponding to the diagonal and the lower/upper triangle of the damping matrix will be needed. Moreover, the block structure of the element shape function matrix, $\mathbf{S}$, substantially reduces the amount of data that has to be stored since each block has only a single associated characteristic value. The invariants of the damping forces, together with those of the elastic forces [12] and the mass matrix, constitute the set of invariants to be calculated during the pre-processing.

3.2.2. *Jacobian of the Damping Forces and Dissipated Power*

The use of implicit integrators requires calculating the Jacobian of the equation of motion. The Jacobian matrix can be calculated numerically from difference formulae. However, numerical differentiation involves a vast effort as it requires a number of function evaluations. It is always more convenient to analytically differentiate the Jacobian if it is possible. The absolute nodal coordinate formulation leads to a very simple expression for the Jacobian of the elastic forces [12]. The Jacobian of damping forces can also be analytically obtained in a very straightforward manner.

The damping force vector depends on both the nodal coordinates by virtue of geometrically nonlinear deformation being considered and also on the nodal velocities. For this reason, the partial derivatives with respect to the nodal coordinates and nodal velocities are required to evaluate the Jacobian of the equations of motion. Based on the simple structure of the invariant formulation described in the previous sub-section, the partial derivative with respect to the nodal coordinates can be evaluated without the need to integrate over the element volume:

$$\left(\frac{\partial \mathbf{Q}_{\mathrm{d}}}{\partial \mathbf{e}}\right)_{ik} = -\sum_{j=1}^{N_{\mathrm{nc}}}\sum_{m=1}^{N_{\mathrm{nc}}} e_m\left(C_{mk}^{ij} + C_{km}^{ij}\right)\dot{e}_j, \tag{28}$$

where $C_{mk}^{ij}$ is the component in row $m$ and column $k$ of the invariant matrix corresponding to position $ij$ in the damping matrix $\mathbf{C}(\mathbf{e})$ and $N_{\mathrm{nc}}$ is the number of absolute nodal coordinates. On the other hand, the partial derivative with respect to the nodal velocities can be written as:

$$\left(\frac{\partial \mathbf{Q}_{\mathrm{d}}}{\partial \dot{\mathbf{e}}}\right)_{ik} = -\mathbf{e}^{\mathrm{T}}\mathbf{C}^{ik}\mathbf{e}. \tag{29}$$

The availability of an exact expression for the partial derivatives of the damping force vector is a valuable feature as it simplifies the evaluation of the Jacobian of the equations of motion. In fact, evaluating the Jacobian is one of the most numerically expensive tasks when using an implicit integrator. In addition, numerical differentiation can result in numerical errors and decrease the convergence rate of the iterative procedure used as a consequence.

Finally, the dissipated power in the proposed internal damping model can be evaluated from the invariants as follows:

$$P_{\mathrm{d}} = \frac{1}{2}\dot{\mathbf{e}}^{\mathrm{T}}\mathbf{C}(\mathbf{e})\dot{\mathbf{e}}. \tag{30}$$

### 3.3. Determination of Damping Coefficients

Experimental values for the damping factors $\gamma_{\mathrm{s}}$ and $\gamma_{\mathrm{d}}$ can be found in the literature [11]; occasionally, however, no data for the specific material used in the model is available. In such a case, one can determine the factors by standard material testing of 'rubber-like' materials (with the viscoelastic material model), which requires experimental work. Dissipation factors can thus be obtained through testing and the application of simple formulae relating the coefficients with some parameters characteristic of the test such as the load application frequency, the boundary conditions of the experiment, etc. [19]. As a result, the values of these viscous damping factors will depend on the frequency range where the tests are conducted and the original problem is expected to operate. In any case, dependence is not too strong as a plot of the viscous damping factor *versus* frequency is an almost horizontal line in the vicinity of the experimental frequency [19].

In any case, it would be useful to find approximate analytical values for the dissipation factors. Hence, no experimental work is needed and the simulation stage can be relieved. In this section, an analytical approximate expression for the dissipation factors is presented. Its derivation is quite straightforward and, although it is an approximation, it provides good results and allows the system to be simulated without the need for any experimental testing.

As stated in the Introduction, a Kelvin–Voigt viscoelastic material model has been used to characterize hysteretic behavior, since, as shown in the literature on damped mechanical vibrations [19, 11], a pure hysteretic model cannot be used in time simulation procedures (complex numbers force frequency domain analysis). Let us assume a unidirectionally deformed material. The hysteretic material, in this case, can be characterized adding an imaginary part to the constant that relates strain and stress (the Young modulus) as follows:

$$\sigma = E(1 + i\delta)\varepsilon, \tag{31}$$

where $i = \sqrt{-1}$ and $\delta$ is the hysteretic damping coefficient. Because this model cannot be used in formulations intended for the simulation of problems in time, an equivalent viscoelastic material model is used and represented by the following expression for the same unidirectional problem:

$$\sigma = E(\varepsilon + \gamma\dot{\varepsilon}), \tag{32}$$

where $\gamma$ is the viscoelastic damping factor and the over-dot denotes derivation with respect to time. Let us assume that the unidirectional problem at hand is the vibration of a beam subjected to a set of boundary conditions at its ends. As shown elsewhere [11, 20], the critical viscoelastic damping factor for the system is given by

$$\gamma_{\mathrm{crit}} = \frac{2}{\omega_{\mathrm{n}}}, \tag{33}$$

where $\omega_n$ is one of the natural frequencies of the vibrating system (with the corresponding boundary conditions). At this point, it is usual to assume the viscous damping constant to be a fraction $\xi$ of critical damping. In order to calculate $\gamma_s$ and $\gamma_d$, we seek for simple configurations of our system giving rise to stress expression similar to that of Equation (32). In such a case, critical damping can be calculated in the same way as in Equation (33). We shall henceforth call these simple configurations "test problems". This procedure was previously applied by Valverde et al. [21] to a Euler beam. In their model, axial/bending and torsion forces were uncoupled. Therefore, the damping factors corresponding to each of these forces do not depend on each other and can be calculated as explained above (pure axial/bending test problem for $\gamma_s$ and pure torsion problems for $\gamma_d$). However, because we have used a continuum mechanics approach to derive the internal forces of the ANCF elements, axial, bending and torsion forces are fully coupled. Therefore, $\gamma_s$ and $\gamma_d$ cannot be calculated separately as they must bear a mutual relation that will be established later on in this section.

Two important facts must be taken into account when computing the analytical equivalent viscous damping factors, namely: (1) the viscous damping factor depends on the frequency of operation of the system, not the original hysteretic material; and (2) the boundary conditions affect the calculation of the critical viscous damping. Here, we propose to calculate the damping factors, $\gamma_s$ and $\gamma_d$ by using appropriate equivalent test problems that allow critical damping to be computed analytically. Because the viscous damping coefficients are frequency-dependent, the analyst must be careful and use them over operational range near the frequency of calculation, which should be the nearest natural frequency of the system to the frequency of application of the loads. Calculating critical damping entails imposing a set of boundary conditions to the test problem. At this point, it is recommended to use boundary conditions as similar as possible to those of the original problem.

Based on Equation (18), a pure deviatoric problem (pure torsion) only implies $\gamma_d$. Taking into account that axis $x$ in the finite element frame points in the direction of the element center-line, a pure torsion problem will obey the following stress–strain relations [22]:

$$\begin{aligned} \sigma_{xx} &= \sigma_{yy} = \sigma_{zz} = \sigma_{yz} = 0, \\ \sigma_{xy} &= 2G\varepsilon_{xy} + 2G\gamma_d\dot{\varepsilon}_{xy}, \\ \sigma_{xz} &= 2G\varepsilon_{xz} + 2G\gamma_d\dot{\varepsilon}_{xz}, \end{aligned} \tag{34}$$

where the following equality for the shear stresses must be fulfilled:

$$\sigma_{xy} = -\sigma_{xz}. \tag{35}$$

Taking into account that shear stresses have the same form as Equation (32), factor $\gamma_d$ can be calculated as a fraction of the critical damping, which can be easily determined by using an expression similar to (33) as

$$\gamma_d^{\text{crit}} = \frac{2}{\omega_n^d}, \tag{36}$$

where $\omega_n^d$ is the corresponding torsional natural frequency of the test problem (a configuration with boundary conditions as similar as possible to those of the original problem). Finally, factor $\gamma_d$ is estimated as a fraction $\xi$ of $\gamma_d^{\text{crit}}$.

On the other hand, a pure longitudinal problem (viz. axial loads or bending loads giving rise to stress in the axial direction) in the direction $x$ gives rise to the following stresses:

$$\sigma_{xx} \neq 0, \quad \sigma_{yy} = \sigma_{zz} = \sigma_{xy} = \sigma_{xz} = \sigma_{yz} = 0, \tag{37}$$

where $\sigma_{xx}$ depends on both $\gamma_\mathrm{s}$ and $\gamma_\mathrm{d}$, see Equation (18). We seek for an expression of $\sigma_{xx}$ equivalent to that of Equation (32):

$$\sigma_{xx} = E\varepsilon_{xx} + E\gamma_{xx}\dot{\varepsilon}_{xx}. \tag{38}$$

In such a case, the factor $\gamma_{xx}$ can be easily calculated in the same way as $\gamma_\mathrm{d}$, i.e. as a fraction $\xi$ of the critical damping given by

$$\gamma_{xx}^{\mathrm{crit}} = \frac{2}{\omega_\mathrm{n}^{xx}}, \tag{39}$$

where $\omega_\mathrm{n}^{xx}$ is the natural frequency of the test problem concerned (a bending or axial vibration frequency depending on wether bending or axial forces, respectively, predominate in the original problem). Once $\gamma^{xx}$ has been obtained from the test problem, the volumetric viscous damping factor $\gamma_\mathrm{s}$ can be obtained equating $\sigma_{xx}$ with (38). Previously, $\sigma_{xx}$ must be expressed in terms of $\varepsilon_{xx}$ and $\dot{\varepsilon}_{xx}$. A relation of $\varepsilon_{yy}$, $\varepsilon_{zz}$ and their time derivatives with $\varepsilon_{xx}$ and its time derivative is therefore needed. Let us use the following expressions from Equation (37):

$$\begin{aligned}\sigma_{yy} = 0 = &\left(K + \frac{4G}{3}\right)\varepsilon_{yy} + \left(K - \frac{2G}{3}\right)(\varepsilon_{xx} + \varepsilon_{zz}) \\ &+ \left(\gamma_\mathrm{s}K + \frac{4\gamma_\mathrm{d}G}{3}\right)\dot{\varepsilon}_{yy} + \left(\gamma_\mathrm{s}K - \frac{2\gamma_\mathrm{d}G}{3}\right)(\dot{\varepsilon}_{xx} + \dot{\varepsilon}_{zz}),\end{aligned} \tag{40}$$

$$\begin{aligned}\sigma_{zz} = 0 = &\left(K + \frac{4G}{3}\right)\varepsilon_{zz} + \left(K - \frac{2G}{3}\right)(\varepsilon_{xx} + \varepsilon_{yy}) \\ &+ \left(\gamma_\mathrm{s}K + \frac{4\gamma_\mathrm{d}G}{3}\right)\dot{\varepsilon}_{zz} + \left(\gamma_\mathrm{s}K - \frac{2\gamma_\mathrm{d}G}{3}\right)(\dot{\varepsilon}_{xx} + \dot{\varepsilon}_{yy}).\end{aligned} \tag{41}$$

A combination of factors $(\varepsilon_{yy} + \varepsilon_{zz})$ and $(\dot{\varepsilon}_{yy} + \dot{\varepsilon}_{zz})$ can be obtained in terms of a combination of $\varepsilon_{xx}$ and $\dot{\varepsilon}_{xx}$ provided $\gamma_\mathrm{s}$ and $\gamma_\mathrm{d}$ are identical. Instead of assuming $\gamma_\mathrm{s} = \gamma_\mathrm{d}$, the following idea can be used: let $\varepsilon$ be the deformation of a solid under a set of applied loads, which in general can usually be considered a periodic function in time with a characteristic frequency $\omega$. In such a case, the deformation can be expressed as [11]

$$\varepsilon \simeq f(\omega t), \tag{42}$$

so:

$$\dot{\varepsilon} \simeq \omega f(\omega t) \simeq \omega\varepsilon. \tag{43}$$

This allows, the following approximation to be made

$$\gamma\dot{\varepsilon} \simeq \gamma\omega\varepsilon \simeq 2\xi\frac{\omega}{\omega_\mathrm{n}}\varepsilon. \tag{44}$$

Because the system is expected to operate at frequencies similar to $\omega_n$ and $\xi < 0.1$, the following inequality can be expected to hold:

$$\gamma \dot{\varepsilon} \ll \varepsilon, \tag{45}$$

so the time derivatives of the deformations in Equations (40) and (41) can be assumed negligible. In such a case, the factor $(\varepsilon_{yy} + \varepsilon_{zz})$ can be expressed in terms of $\varepsilon_{xx}$ as

$$(\varepsilon_{yy} + \varepsilon_{zz}) = -\frac{3K - 2G}{3K + G}\,\varepsilon_{xx}. \tag{46}$$

By differentiating Equation (46) with respect to time one obtains

$$(\dot{\varepsilon}_{yy} + \dot{\varepsilon}_{zz}) = -\frac{3K - 2G}{3K + G}\,\dot{\varepsilon}_{xx}. \tag{47}$$

Substituting relations (46) and (47) into the expression of $\sigma_{xx}$ given by (18), the following is obtained

$$\sigma_{xx} = \frac{9KG}{3K + G}\,\varepsilon_{xx} + \frac{\gamma_s + 2\gamma_d}{3}\,\frac{9KG}{3K + G}\,\dot{\varepsilon}_{xx}. \tag{48}$$

A comparison of Equations (38) and (48), allows the following relation between $\gamma_{xx}$, $\gamma_s$ and $\gamma_d$ to be formulated:

$$\gamma_{xx} = \frac{\gamma_s + 2\gamma_d}{3}, \tag{49}$$

In summary, the process involves the following steps: (1) choosing a test problem with boundary conditions as similar as possible to those of the original problem and simple enough to allow the natural frequencies to be determined. (2) Calculating $\gamma_d$ by using a torsional natural frequency suited to the frequency of application of torsional forces. Equation (36) must be used for this purpose. (3) Calculating $\gamma_{xx}$ by using Equation (39). A bending or axial natural frequency must be chosen that should be as close as possible to that of the applied forces. (4) Finally, calculating $\gamma_s$ by using Equation (49). An appropriate factor $\xi$ must be chosen by the analyst for both viscous damping constants suited to the nature of the target problem.

By way of example, the problem of the SET can be used [1]. This configuration is similar to a clamped beam with a vast mass at its free end. In this problem, the clamped end its subjected to a constant angular velocity and the structure transversal vibration is mainly due to bending forces. In such a case, $\gamma_{xx}$ should be calculated by using the first bending natural frequency of the clamped beam with a mass at its free end with conservation of the boundary conditions. $\gamma_d$ is calculated by using the first torsional natural frequency for the same configuration.

For more general multibody problems, it is well known that the determination of the natural frequency is a complex task, as it depends on the position of the system in time. Besides, the boundary conditions of the flexible bars would also depend on the given position of the multibody system. In such a case, it would be interesting to calculate the natural frequencies for different positions, the most different ones in terms of boundaries for the flexible bars. Then, the analyst can decide if the range of frequencies is large enough to consider a mean natural frequency along the motion of the mechanism. In any case, the analyst must be aware of the approximate nature of the proposed calculation of the damping factors, therefore, in some cases it would not be necessary to go to a very exact calculation of the natural frequencies.

## 4. Non Dissipation Under Rigid Body Motion

Multibody systems can experience deformations as well as rigid body motion. It is therefore essential for all internal damping models not to dissipate energy under conditions of rigid body motion. In the absolute nodal coordinate formulation, rigid body motion can be accomplished by using appropriate shape functions (i.e. accurately representing rigid body motion [10, 13]). This however, does not ensure that rigid body motions will not be damped out.

As can be inferred from Equation (22), the proposed internal damping model produces zero damping forces if deformation rates are all zero, this is a result of all terms in equation being multiplied by a component of the deformation rate tensor. Furthermore, when the Green–Lagrange nonlinear strain–displacement relationship is used to measure deformations and deformation rates, deformation rates are always zero for rigid body motion. This can be demonstrated by assuming the global position of an arbitrary point in a body under rigid body motion to be described by the following expression:

$$\mathbf{r} = \mathbf{R} + \mathbf{A}\mathbf{x}, \tag{50}$$

where $\mathbf{R}$ is the global position of the point in the solid, $\mathbf{A}$ an orthogonal rotation matrix and $\mathbf{x}$ the position of the arbitrary point in the body reference frame. Provided Equation (50) holds, the deformation gradient can be expressed as follows:

$$\mathbf{J} = \frac{\partial \mathbf{r}}{\partial \mathbf{r}_0} = \frac{\partial \mathbf{r}}{\partial \mathbf{x}}\left[\frac{\partial \mathbf{r}_0}{\partial \mathbf{x}}\right]^{-1} = \mathbf{A}\mathbf{A}_0^{-1}, \tag{51}$$

where $\mathbf{A}_0$ is the constant orthogonal rotation matrix corresponding to the reference configuration. From Equation (51), the time derivative of the Green–Lagrange strain tensor can be expressed as follows:

$$\dot{\varepsilon} = \frac{1}{2}(\dot{\mathbf{J}}^{\mathrm{T}}\mathbf{J} + \mathbf{J}^{\mathrm{T}}\dot{\mathbf{J}}) = \frac{1}{2}\left(\mathbf{A}_0^{-1}\right)^{\mathrm{T}}(\dot{\mathbf{A}}^{\mathrm{T}}\mathbf{A} + \mathbf{A}^{\mathrm{T}}\dot{\mathbf{A}})\mathbf{A}_0^{-1}. \tag{52}$$

Because the rotation matrix, $\mathbf{A}$, is orthogonal,

$$\mathbf{A}^{\mathrm{T}}\mathbf{A} = \mathbf{I}. \tag{53}$$

Differentiating both sides of Equation (53) once with respect to time therefore yields

$$\dot{\mathbf{A}}^{\mathrm{T}}\mathbf{A} + \mathbf{A}^{\mathrm{T}}\dot{\mathbf{A}} = \mathbf{0}, \tag{54}$$

which coincides with the term in brackets on the right hand side of Equation (52). Thus, $\dot{\varepsilon}$ is zero under rigid body motion. Therefore, the requirement that no energy should be dissipated under rigid body motion is automatically met if the nonlinear Green–Lagrange strain–displacement relationship is used to evaluate the time derivatives of the strain tensor.

## 5. Numerical Examples

The proposed internal damping force model was validated by solving three numerical examples. In the first example, the formulation was checked against a well-established reference frame formulation

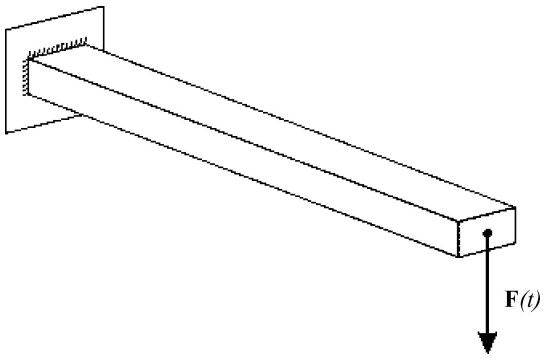


*Figure 2.* Cantilever beam subjected to a concentrated force at its free end.

based on natural coordinates [1, 3, 23] and substructuring [24] that accounts for geometric nonlinearity. Small and large deformation problems were solved in order to compare the numerical results. In the second example, the motion of a flexible beam was simulated in order to show that the translational rigid body motion of the beam is not damped out. The third example involved rotating the previous beam about one of its axes. In this simulation, rotational rigid body motion was not damped out.

### 5.1. Example 1

The problem of a cantilever beam subjected to a concentrated load at its free end was analysed here. The beam was modelled by using a total 16 three-dimensional beam elements based on absolute nodal coordinates [10]. Figure 2 illustrates the problem at hand. The load was applied to the beam by starting from zero and reaching a final value $f_{t_c}$ at time $t_c$. The length of the beam was assumed to be 5 m and the cross-section to be square with $h = w = 0.1$ m (height and width). Also, the beam material was assumed to have a Young's modulus of $1.32\times10^{11}$ N/m$^2$ and a density 8245.2 kg/m$^3$. As recommended by Sopanen et al. [25], Poisson's ratio was assumed to be 0 in order to avoid the inherent overly stiff behavior of the beam element used [10]. Also, the damping factors, $\gamma_s$ and $\gamma_d$ were computed by following the procedure described above. This entailed calculating the natural frequencies (torsion and bending) of the beam. The first torsion natural frequency of the system was

$$\omega_n^d = \alpha\sqrt{\frac{CG}{\rho L^2 I_p}}, \tag{55}$$

where $\alpha = \frac{\pi}{2}$ for the boundary conditions at hand, $C = 0.1406h^4$ is the torsion factor of a square cross-section, $G$ the shear modulus of the beam material and $I_p = 2I$ the polar moment of the cross-section. Therefore, if 5% of the critical damping is assumed, the deviatoric damping coefficient will be given by expression (36). On the other hand, the first bending natural frequency of the system will be

$$\omega_n^b = \beta\sqrt{\frac{EI}{mL^3}} = \omega_n^{xx}, \tag{56}$$

where $\beta = 1.875^2$ for the boundary conditions at hand, $I = \frac{h^4}{12}$ is the second moment of area of the cross-section and $m = \rho h^2 L$ the beam mass. Parameter $\gamma_{xx}$ is assumed the 5% of the critical one, given by expression (39). Once $\gamma_d$ and $\gamma_{xx}$ have been determined, $\gamma_s$ can be obtained from Equation

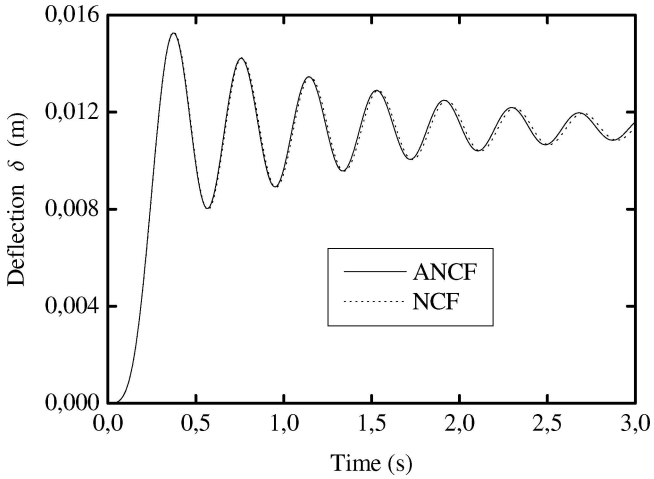


*Figure 3.* Deflection of the beam tip (small deformations).

(49). First, a force small enough to cause small deformations is applied to the beam. The characteristic values of the applied force were $t_c = 0.35$ s and $f_{t_c} = 300$ N and the expected final sag of the beam $\delta = 1.14 \times 10^{-2}$.

As can be seen in Figure 3, the solutions provided by both procedures (ANCF and natural coordinate formulation, NCF) were quite consistent. A total of 12 substructures were used to model the beam with the natural coordinate formulation. At long simulation times, the deflection $\delta$ levelled off at the above-described value, once vibration around the elastic equilibrium was damped out by internal damping forces.

The force applied to the system was now increased, so the deformations experienced by the beam could be assumed to be large ($t_c$ and $f_{t_c}$ were assumed to be 0.6 s and 60 000 N, respectively). The deflection of the free end of the beam was unknown *a priori*. The simulation results provided by the two models (ANCF and NCF) are shown in Figure 4. Consistency was quite good and the final deflection $\delta \approx 20\%L$. Figure 5, which is a magnified view of Figure 4 around elastic equilibrium, reveals that

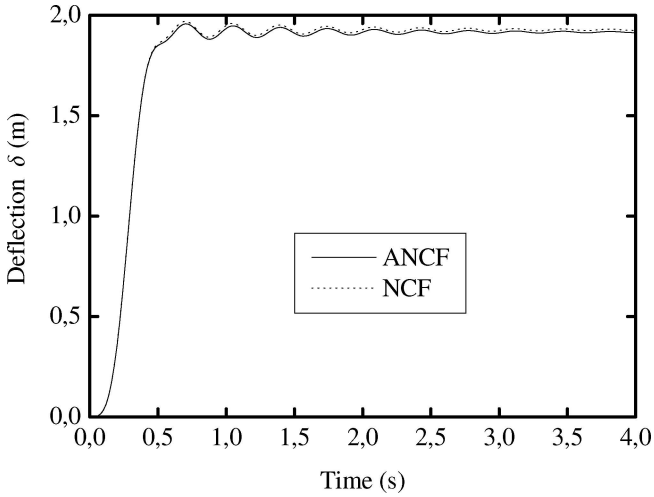


*Figure 4.* Deflection of the beam tip (large deformations).

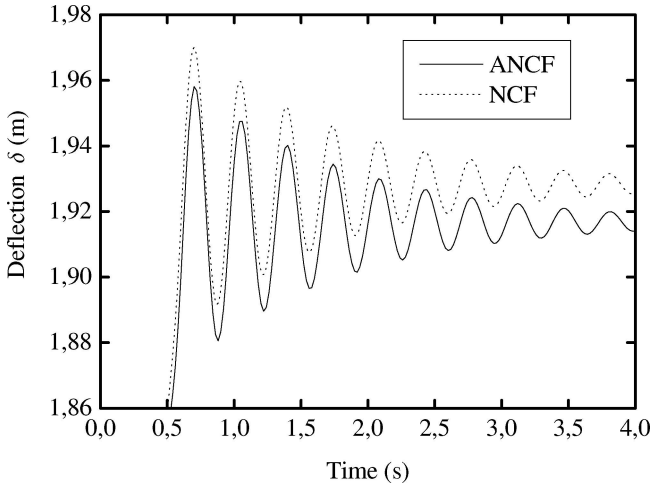


*Figure 5*. Deflection of the beam tip (magnified view of Figure 4).

both models dissipate energy in the same way: vibration around elastic equilibrium is damped out similarly, so the periodicity of both solutions is identical. There is a small difference, about 0.5% of the total deflection, which was also encountered in the problem involving small deformations and can be ascribed to the different modelling scheme used in the two models.

### 5.2. Example 2

The problem involves an upright flexible beam that is horizontally thrown in the absence of gravity forces (the flying beam). This problem was previously studied by Takahashi et al. [6] to check their Rayleigh-like damping model. Figure 6 illustrates the problem and the time dependence of the applied load.

The beam was assumed to have a length $L = 8$ m, a cross-sectional area $A = 0.0307$ m$^2$ and a second moment of area $I = 7.854 \times 10^{-5}$ m$^4$. The beam material was assumed to have a volumetric density $\rho = 7860\,\mathrm{kg/m^3}$ and a Young's modulus $E = 2.10$ GPa. The beam, initially straight, was

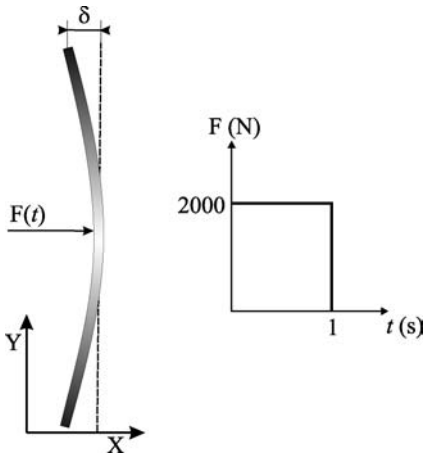


*Figure 6*. The flying beam problem.

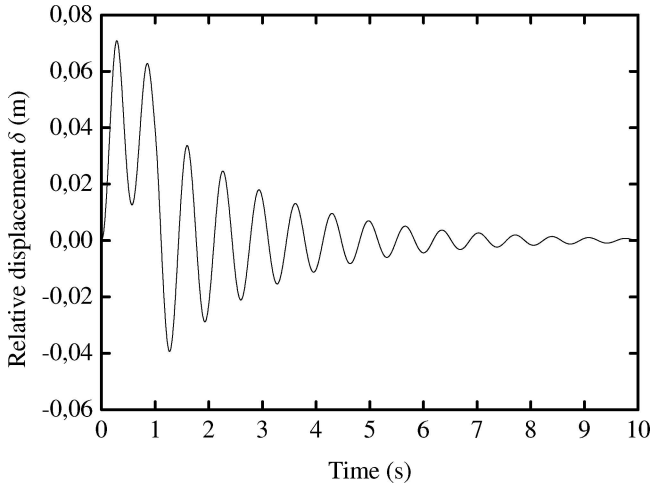


*Figure 7.* Relative displacement between the center of mass and the tip of the flying beam.

discretized by using 8 two-dimensional shear deformable elements [9]. The position of the beam at time $t = 0$ s coincided with the $Y$ global axis, with one of the ends over the origin of the coordinate system. Damping coefficients were computed from the first torsion and bending natural frequencies of a beam with boundary conditions of free ends. The first natural torsion frequency of a free-free beam was used to calculate the deviatoric damping coefficient, $\gamma_{\mathrm{d}}$. The torsion natural frequency was given by Equation (55), where, for the boundary conditions of this example, $\alpha = \pi$ and the constants $C$, $G$, $I_{\mathrm{p}}$ were defined in the first example. If the beam cross-section is square, then: $C = 0.1406h^4$ with $h = \sqrt{A}$, $G = \frac{E}{2(1+\nu)}$, where $\nu = 0$, and $I_{\mathrm{p}} = 2I$. Therefore, the deviatoric damping coefficient is given by Equation (36) multiplied by the coefficient $\xi = 0.05$. On the other hand, the fundamental bending frequency is given by Equation (56) with $\beta = 4.73^2$. Therefore, $\gamma_{xx}$ is given by expression (39) with $\xi = 0.05$. Again, $\gamma_{\mathrm{s}}$ can be calculated from Equation (49).

Figure 7 shows the relative displacement, $\delta$, between the midpoint and a line connecting both ends of the flying beam (Figure 6), which is a measure of deformation in the beam. As can be seen in the figure, deformation peaked near the end of the loading process. After the load was removed, displacements due to deformation decreased to near zero through dissipation resulting from internal damping forces. The logarithmic decrement method [15] was used to estimate the damping ratio. Based on the results of Figure 7, an average damping ratio of 0.0503, which is quite close to the 0.05 assumed was obtained. This confirms that the criteria explained in Section 3.3 to estimate the dissipation factors provided the expected results.

Figure 8 shows the velocity of the midpoint of the beam and the center of mass of a similar rigid beam as a function of time. The figure shows how the velocity of the midpoint of the flexible beam tends to that of the center of mass of the rigid beam. This is so because the momentum of the beam must be preserved in absence of external forces and the only difference between both models are the internal elastic and damping forces. Figure 8 therefore demonstrates that the proposed damping model in the present paper does not affect rigid body translations.

Finally, Figure 9 shows the balance of energy in the flying beam problem. The kinetic and strain energies of the beam are shown. Initially, while the load is being applied, the total energy increases. Once the strain energy has been dissipated by the damping forces, the total energy reaches a constant value corresponding to the constant velocity of the beam, which is in turn equal to the velocity of the rigid beam case. The kinetic energy remains constant also because the proposed damping model only

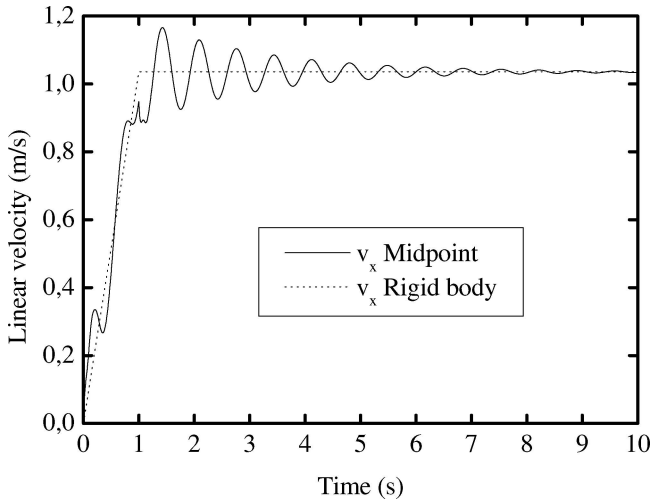


*Figure 8.* Velocity of the center of mass of the flying beam (rigid and flexible cases).

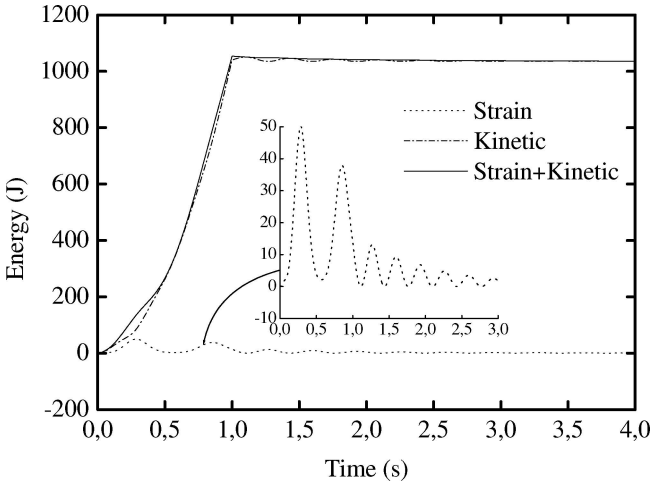


*Figure 9.* Balance of energy in the flying beam problem.

dissipates the strain energy of the flexible beam. After the strain energy is dissipated, the beam only possesses kinetic energy due to rigid body translation.

The influence of the different damping ratios can be seen in Figure 10. As the damping ratio is increased, the system is damped out faster and the frequency of vibration of the beam, which depends on the damping ratio, decreases.

### 5.3. Example 3

In the previous example, the translational motion of a flexible beam was used to show that the internal damping model is dissipating no energy from the rigid body motion. In this example, an identical conclusion is reached for a flexible beam subjected to pure rotation about an orthogonal axis passing through one of its ends. Figure 11 depicts of the flexible beam and its boundary conditions.

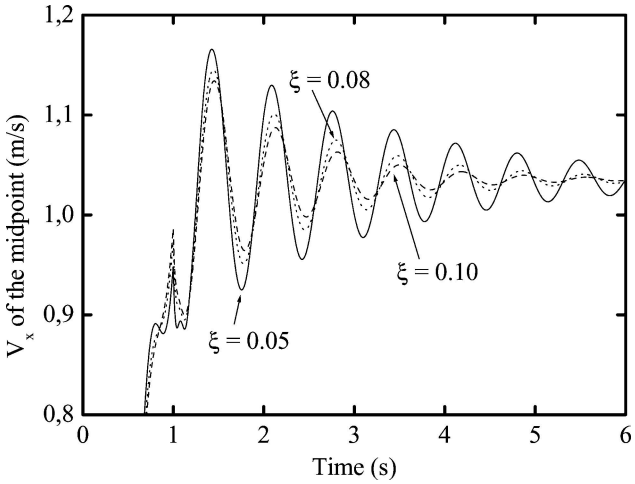


*Figure 10.* Influence of the damping ratio, $\xi$.

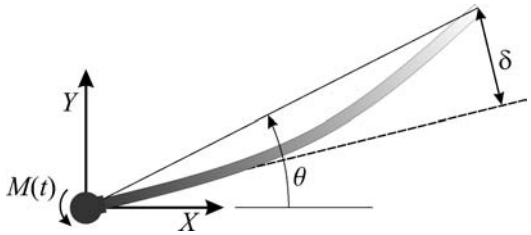


*Figure 11.* Flexible beam subjected to a concentrated moment.

The beam had the same properties as that of the previous example. A revolute joint between the beam and a fixed reference was placed at one end. In order to estimate the damping parameters, the fundamental frequencies of a hinged-free beam was used at a damping ratio of 0.05. The torsion fundamental frequency used was that of Equation (55) for the cantilever beam problem and the bending fundamental frequency for the hinged-free beam was that of Equation (56) with $\beta = 3.93^2$. Again, the damping factors were evaluated as described in Section 3.3. The moment applied at $t = 0$ s was 5000 N m and removed after 2 s. Figure 12 shows the deflection of the free end of the beam as measured in a local frame attached to the hinged end of the beam. As expected, the amplitude of the oscillations start to decrease when the external concentrated moment cancelled.

In order to check that rigid rotation of the beam was not damped, a rigid beam with the same geometric properties and density was studied. In this simulation, the nodal coordinates and nodal velocities of the end node were used to calculate the velocity of rotation of the node. If the node position is expressed in a polar coordinate system, then the angular coordinate can be expressed as follows:

$$\theta = \tan^{-1} \frac{r_2}{r_1}, \tag{57}$$

where $r_1$ and $r_2$ are the global coordinates of the node. From Equation (57), it follows that the time derivative of the angular coordinate, $\theta$, can be expressed as follows:

$$\dot{\theta} = \frac{\dot{r}_2 r_1 - \dot{r}_1 r_2}{r_1^2 + r_2^2}, \tag{58}$$

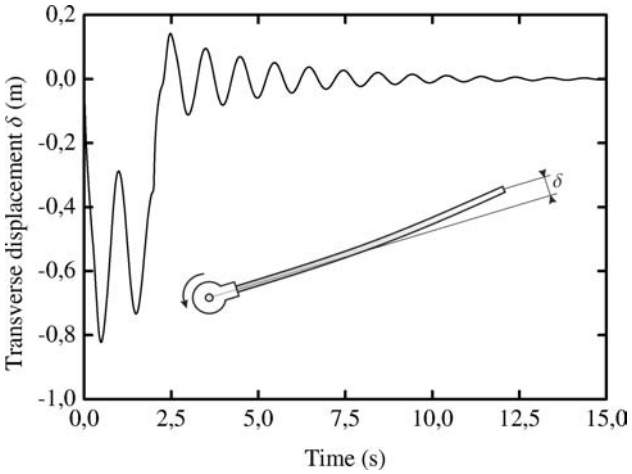


*Figure 12*. Deflection of the free end.

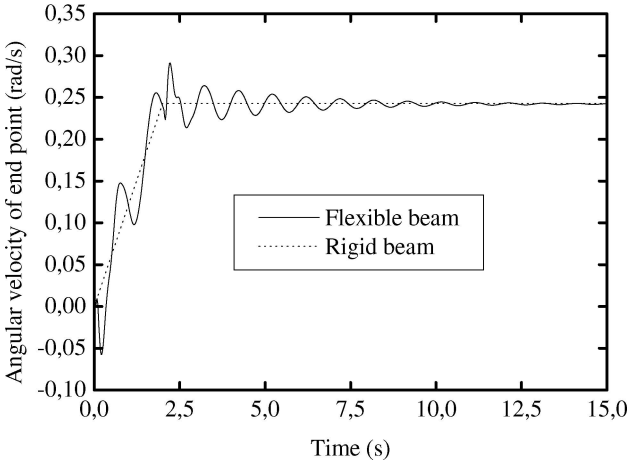


*Figure 13*. Angular velocity, $\dot{\theta}$, of the end node.

Figure 13 shows the variation of the time derivative of the angular coordinate, $\dot{\theta}$, of the free end of the beam with the angular velocity of the rigid beam. As can be seen, the angular velocity of the rigid beam increases linearly while the applied moment remains constant. When the applied moment cancels, the angular velocity of the rigid beam remains constant. The time derivative of the angular coordinate of the end node in the polar coordinate system exhibits a similar behavior. After oscillations are damped out, $\dot{\theta}$ and the angular velocity of the rigid beam coincide as a result of the flexible beam rotating like a rigid beam. As a consequence, the time derivative of the angular coordinate, $\dot{\theta}$, at every point of the flexible beam is the same and coincides with the angular velocity of the rigid beam. Therefore, some time after the moment is removed, the flexible beam continues to rotate as a rigid body.

Finally, Figure 14 shows the variation of the elastic and kinetic energies of the rotating flexible beam with time. As in the previous example, elastic energy is dissipated while deformation extinguishes. After some time, the kinetic energy tends to a constant value corresponding to the kinetic energy of the beam under rigid body rotation. In other words, the beam can rotate as a rigid body about the fixed end without any dissipation of energy as rigid body motions are not damped out.

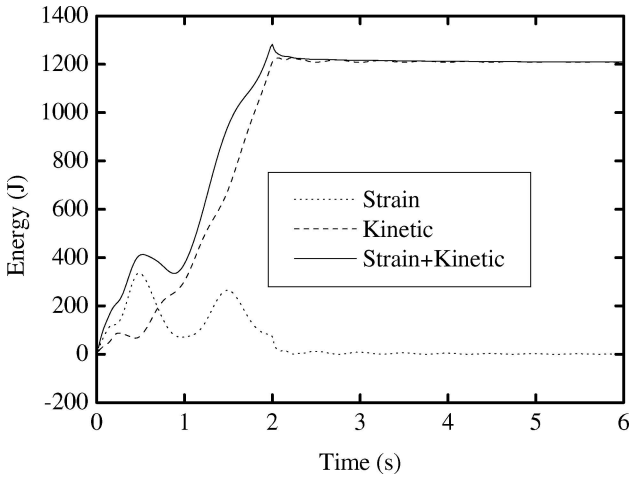


*Figure 14*. Variation of the elastic and kinetic energies with time.

## 6. Conclusions

The main purpose of this paper was to develop an internal damping model for the absolute nodal coordinate formulation, which is a recently reported multibody description for large deformation problems. Properly formulating the model is essential as, in some practical cases, damping has a crucial influence on the behavior of the system concerned. In addition, some recent damping models fail to provide a close description of internal damping in the material as they dissipate energy during rigid body motions.

In this work, internal damping was modelled on the assumption that the material behaves as an equivalent viscoelastic one, which is a common practice in engineering when time simulations are required [11]. Also, viscous damping was adapted to a continuum mechanics approach in a systematic, straightforward manner. Elastic and damping forces were thus obtained in a similar way, taking advantage of the presence of some invariant quantities that have to be calculated only once at the pre-processing stage of the simulation [12].

Because damping forces are evaluated by using a continuum mechanics approach, geometric nonlinearity is taken into account. Also, the proposed damping model can be applied to large deformation problems as it involves no assumptions on deformations. Other damping formulations for the ANCF [6, 7] require small deformations within each finite element and manipulation of elastic forces in order to separate bending and axial deformations with a view to formulating a Rayleigh-like damping model; this detracts from generality in such models.

Data for specific materials in relation to the viscous damping model used, which is based on two material constants ($\gamma_s$ and $\gamma_d$) have been reported elsewhere [11]. Even if the material used with the model has not been characterized previously, the damping constants can be obtained by conducting some simple experimental tests. When experimental work is unfeasible, the damping constants can be calculated by using the proposed analytical approximation based on several basic test problems involving vibration in a system under similar boundary conditions as the actual problem to be solved. The results obtained by using these analytically obtained damping constants can be very useful at an early stage in designing a mechanism. In fact, they allow damping factors to be accurately calculated with minimal effort. Accuracy is even greater if experimental data for the model concerned is available.

As shown by the first example, the proposed model provides good results relative to such a well-established formulation as NCF with both small and large deformation problems. Non-dissipation in rigid body motions was demonstrated both analytically and numerically.

## Acknowledgement

The authors thank the Spanish Ministry of Science and Technology for the support of part of this work.

## References

1. Valverde, J., Escalona, J. L., Mayo, J., and Domínguez, J., 'Dynamic analysis of a light structure in outer space: Short Electrodynamic Tether', *Multibody System Dynamics* **10**(1), 2003, 125–146.
2. Shabana, A. A., *Dynamics of Multibody Systems*, 2nd edn., Cambridge University Press, 1998.
3. García de Jalón, J. and Bayo, E., *Kinematic and Dynamic Simulation of Multibody Systems – The Real-Time Challenge*, Springer–Verlag, New York, 1993.
4. Simo, J. C. and Vu-Quoc, L., 'On the dynamics of flexible beams under large overall motions – The plane case: Part I and Part II', *ASME Journal of Applied Mechanics* **53**, 1986, 849–863.
5. Escalona, J. L., Hussien, H. A., and Shabana, A. A., 'Application of the absolute nodal coordinate formulation to multibody system dynamic', *Journal of Sound and Vibration* **214**(5), 1998, 833–951.
6. Takahashi, Y., Shimizu, N., and Suzuki, K., 'Introduction of damping matrix into absolute coordinate formulation', in *Proceedings of the Asian Conference on Multibody Dynamics*, Iwaki, Fikushima, 2002, pp. 33–40.
7. Yoo, W., Lee, J., Sohn, J., Park, S., Dmitrochenko, O., and Pogorelov, D., 'Comparison of physical experiments and computer simulation with ANCF: Large deformation of a thin cantilever beam', in *Proceedings of the ASME DETC&CIE Conference*, Chicago, IL, 2003.
8. Novozhilov, V. V., *Foundations of the Nonlinear Theory of Elasticity*, 2nd edn., Graylock Press, Rochester, 1957.
9. Omar, M. and Shabana, A. A., 'A two-dimensional shear deformable beam for large rotation and deformation problems', *Journal of Sound and Vibration* **243**(3), 2001, 565–573.
10. Shabana, A. A. and Yakoub, R. Y., 'Three-dimensional absolute nodal coordinate formulation for beam elements: Theory', *ASME Journal of Mechanical Design* **123**, 2001, 606–613.
11. Snowdon, J. C., *Vibration and Shock in Damped Mechanical Systems*, Wiley, New York, 1968.
12. García-Vallejo, D., Mayo, J., Escalona, J. L., and Domínguez, J., 'Efficient evaluation of the elastic forces and the Jacobian in the absolute nodal coordinate formulation', *Nonlinear Dynamics* **35**, 2004, 313–329.
13. Mikkola, A. M. and Shabana, A. A., 'A non-incremental finite element procedure for the analysis of large deformation of plates and shells in mechanical system applications', *Multibody System Dynamics* **9**, 2003, 283–309.
14. Meirovitch, L., *Methods of Analytical Mechanics*, McGraw-Hill, New York, 1970.
15. Ginsberg, J. H., *Mechanical and Structural Vibrations*, Wiley, New York, 2001.
16. Findley, W. N., Lai, J. S., and Onaran, K., *Creep and Relaxation of Nonlinear Viscoelastic Materials*, North-Holland Publishing, 1976.
17. Simo, J. C. and Hughes, T. J. R., *Computational Inelasticity*, Springer-Verlag, New York, 1998.
18. Sugiyama, H. and Shabana, A. A., 'Application of plasticity theory and absolute nodal coordinate formulation to flexible multibody system dynamics', *ASME Journal of Mechanical Design* **126**, 2004, 478–487.
19. Nashif, A. D., Jones, D. I. G., and Henderson, J. P., *Vibration Damping*, Wiley, New York, 1985.
20. Shabana, A. A., *Theory of Vibration, Volume II: Discrete and Continuous Systems*, Springer–Verlag, New York, 1991.
21. Valverde, J., Escalona, J. L., Freire, E., and Domínguez, J., 'Stability and bifurcation analysis of a geometrically nonlinear orthotropic Jeffcott model with internal damping', *Nonlinear Dynamics*, in press.
22. Timoshenko, S. and Goodier, J. N., *Theory of Elasticity*, McGraw-Hill, New York, 1951.
23. Cuadrado, J., Cardenal, J., and García de Jalón, J.,'Flexible mechanisms through natural coordinates and component mode synthesis: An approach fully compatible with the rigid case', *International Journal of Numerical Methods in Engineering* **39**, 1996, 3535–3551.
24. Wu, S. and Haug, E. J., 'Geometric non-linear substructuring for dynamics of flexible mechanical systems', *International Journal for Numerical Methods in Engineering* **26**, 1988, 2211–2226.
25. Sopanen, J. T. and Mikkola, A. M.,'Description of elastic forces in absolute nodal coordinate formulation', *Nonlinear Dynamics* **34**, 2003, 53–74.